Geologica Acta, Vol.7, Nos 1-2, March-June 2009, 229-242
DOI: 10.1344/105.000000280
Available online at www.geologica-acta.com

Rock magnetic properties across the Paleocene-Eocene Thermal Maximum in Marlborough, New Zealand

V. VILLASANTE-MARCOS [1] **C.J. HOLLIS** [2] **G.R. DICKENS** [3] **and M.J. NICOLO** [3]

[1] **Departamento de Geofísica y Meteorología, Facultad de Ciencias Físicas, Universidad Complutense de Madrid**
28040 Madrid, Spain. E-mail: vicvilla@fis.ucm.es

[2] **GNS Science**
PO Box 30-368 Lower Hutt, New Zealand.

[3] **Department of Earth Sciences, Rice University**
Houston, Texas, TX 77005, USA.

ABSTRACT

Rock magnetic properties have been investigated across the Paleocene-Eocene Thermal Maximum (PETM) in three uplifted sections of Paleogene marine sedimentary rocks in Marlborough, South Island, New Zealand. The sections are exposed along Mead Stream, Dee Stream and Muzzle Stream and represent a depth transect up a continental margin from an upper slope to an outer shelf. Sampling was focused on rock beds previously examined for their biostratigraphy and stable carbon isotope ($\delta^{13}C$) composition, and where a prominent clay-rich interval referred to as Dee Marl marks the initial 80-100 kyr of the PETM. Measured magnetic properties include bulk magnetic susceptibility, hysteresis cycles and isothermal remanent magnetization (IRM) acquisition and back-demagnetization curves. A strong inverse correlation between magnetic susceptibility and bulk carbonate $\delta^{13}C$ is found across the PETM such that Dee Marl has low $\delta^{13}C$ and high magnetic susceptibility. At Mead Stream this interval also contains increased saturation-IRM, and thus ferromagnetic content. Rock magnetic behaviour across PETM is best explained by an increase in terrigenous discharge. This inference has been made previously for PETM intervals in New Zealand and elsewhere, although with different proxies. Increased terrigenous discharge probably signifies an acceleration of the hydrological and weathering cycles. Some changes in magnetic phases could also reflect a drop in redox conditions, which could represent higher sedimentation rates, greater input of organic carbon, dysoxic bottom waters, or a combination of all three. A drop in redox conditions has been inferred for other marine sections spanning the PETM.

KEYWORDS | **Magnetic properties. Paleocene-Eocene Thermal Maximum. Terrigenous input. Continental weathering.**

INTRODUCTION

Many studies over the past fifteen years have led to a general understanding of the Paleocene-Eocene Thermal Maximum, typically referred to as the PETM (Bowen et al., 2006). About 55.5 Ma ago, temperatures on Earth's surface, including deep-ocean water, rose by 4-10°C within 20,000 yrs. This warming was associated with a

massive injection of ^{13}C-depleted carbon into the ocean-atmosphere system. Although the source of the carbon remains controversial (e.g., Dickens et al., 1997; Kent et al., 2003; Kurtz et al., 2003; Svensen et al., 2004), it is clearly evidenced by a rapid and pronounced negative carbon isotope ($\delta^{13}C$) excursion in carbon-bearing phases deposited across the globe, and by a prominent carbonate dissolution horizon in deep-sea sediment sequences. Over the next 200,000 years or so, climate and carbon cycling returned to near-initial conditions, although the trajectory for both remains uncertain. Within these ~220,000 years occurred major biotic turnovers on land and in the ocean, including a widespread benthic foraminifera extinction event (BFEE) near the onset. The interval has attracted considerable attention across the broad geoscience community because of obvious analogies to the present-day carbon input and global warming (e.g., Dickens, 1999).

An important issue regarding climate change during the PETM (and in the future) is the response of hydrological and weathering cycles to extreme warming and massive carbon input. Generic models indicate that a rise in Earth surface temperatures should accelerate the global hydrological cycle, increasing evaporation rates in some regions, especially the subtropics, and increasing precipitation rates in other regions, especially at high latitudes (e.g., Allen and Ingram, 2002; Bice and Marotske, 2002). This, together with increased temperature and atmospheric pCO_2 caused by the carbon injection, should increase erosion and weathering on land, particularly in wet regions with enhanced precipitation rates. One might expect, therefore, greater discharge of weathered continental material to the oceans during extreme warmth, especially at high latitudes. A globally accelerated hydrological cycle during the PETM has been inferred from a large positive excursion in the hydrogen isotopes of organic matter deposited in the Arctic (Pagani et al., 2006). Overall enhanced continental weathering and terrigenous derived dissolved Os input to the oceans during the PETM has also been suggested from a major increase in the $^{187}Os/^{186}Os$ ratio of marine sediment across the PETM (Ravizza et al., 2001). Both inferences are supported by elevated siliciclastic sedimentation rates or changes in mineralogy, geochemistry or organic matter along certain continental margins (e.g., Robert and Kennett, 1992, 1994; Schmitz et al., 2001; Crouch et al., 2003; Dickens and Francis, 2004; Hollis et al., 2005a; Giusberti et al., 2007; Nicolo et al., 2007).

Rock magnetic properties are a useful tool for tracking variations in sediment composition, including terrigenous concentration and the type and concentration of ferromagnetic minerals; hence, they can aid in paleoclimatic interpretations (Thompson and Oldfield, 1986; Verosub and Roberts, 1995; Walden et al., 1999; Maher and Thompson, 1999; Evans and Heller, 2003). To our knowledge, however, there have been only few published studies of rock magnetic properties in sediment spanning the PETM (Kent et al., 2003; Lippert et al. 2004, 2007; Kopp et al., 2007). In their paper, Kent et al. (2003) found significant variations across the PETM in three sediment cores from the New Jersey margin. The changes in rock magnetic properties are consistent with a high abundance of single-domain magnetite, which Kent et al. (2003) attributed to comet residue, although enhanced weathering inputs and a drop in depositional redox conditions at a low latitude location could explain the observations (Dickens and Francis, 2004). Later, Lippert et al. (2004, 2007) and Kopp et al. (2007) have presented rock magnetic data across the PETM in several sites, interpreting the properties measured by Kent et al. (2003) as a regional and purely terrestrial feature. The aim of the present study is to examine rock magnetic properties across the PETM in sedimentary sections deposited on a high latitude continental margin in the southern hemisphere, in order to identify changes that might be due to intrinsic climatic processes or extrinsic factors, such as cometary impact.

LOCATION AND SAMPLES

Southeast-running tributaries of Clarence River in Marlborough, South Island, New Zealand (Fig. 1A), cut through uplifted and tectonically rotated marine sedimentary rocks of late Cretaceous to middle Eocene age (Reay, 1993; Strong et al., 1995). This sequence was originally deposited along a north-facing terrigenous-starved continental margin referred to as the "Marlborough paleoembayment"; deposition occurred at a latitude of ~55º S during the late Paleocene (Crampton et al., 2003), a location expected to record significant modulation in the global hydrological cycle.

The spectacularly exposed Upper Paleocene-Lower Eocene sections within Clarence Valley are characterized by well-bedded rocks comprised of three components (Reay, 1993; Strong et al., 1995; Hancock et al., 2003; Hollis et al., 2005a, b): biogenic limestone, biogenic chert, and calcareous claystones (marls). So far, rock sections along three tributaries have been logged in detail, examined for their microfossil assemblages and stable carbon isotope compositions, and placed into global stratigraphic context; these are: Mead Stream, Dee Stream and Muzzle Stream (Strong et al., 1995; Hancock et al., 2003; Hollis et al., 2005a, b). Together, these sections represent a >20 km transect across a continental margin from middle slope (Mead Stream), through upper slope (Dee Stream), to outer shelf (Muzzle Stream). Strike-slip and thrust faults in the region have probably resulted in some shortening. Therefore the

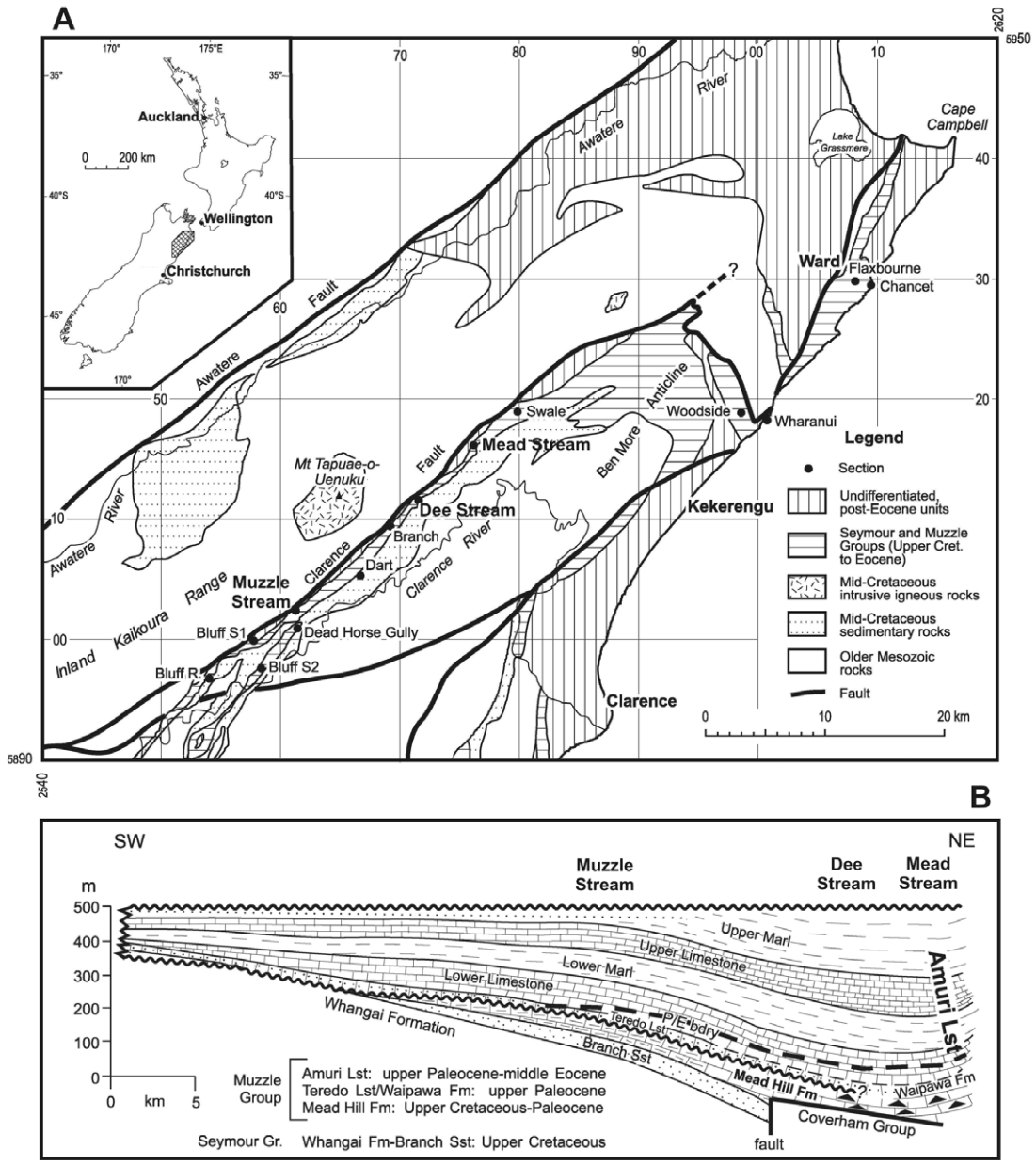

FIGURE 1 | **A) Simplified geological map and geographic location of the three studied sections in the Marlborough region, South Island (New Zealand) (from Hollis et al., 2005a). B) Trends in lithofacies and sedimentary units in Clarence River Valley strata (from Hollis et al., 2005a).**

original depositional distances between the three sites are likely to have been significantly greater than is suggested by their present proximity. In general, depositional depth and thickness increase to the northeast, so that the depocentre for Paleogene sediment lies near Mead Stream (Fig. 1B) (Reay, 1993). The PETM has been clearly identified in all three sections on the basis of changes in microfossil assemblages and stable carbon isotopes (Hancock et al., 2003; Hollis et al., 2005a, b). Notably, approximately the first half of the PETM is marked by a clay-rich unit (Fig. 2), which has been named Dee Marl (Hollis et al., 2005a).

The thickness of the early Paleogene section as well as the Dee Marl varies across the three sections. Specifically, Dee Marl is ~ 2.4 m thick at Mead Stream (157.2-159.4 m), ~ 1 m at Dee Stream (26.05-27.03 m), and ~ 0.8 m at Muzzle Stream (5.3-6.1 m) (Hancock et al., 2003; Hollis et al., 2005a, b). At each location, Dee Marl spans the full drop in $\delta^{13}C$ but not the full recovery in $\delta^{13}C$ (Figs. 3, 4 and 5). The full drop in $\delta^{13}C$ spans about 80-100 kyr on the basis of work elsewhere (Bowen et al., 2006; Giusberti et al., 2007). Consequently, compacted sedimentation rates for the initial part of the PETM are approximately 2.4-3.0 cm/kyr at Mead Stream, 1.0-1.3 cm/kyr at Dee Stream, and 0.8-1.0 cm/kyr at Muzzle Stream.

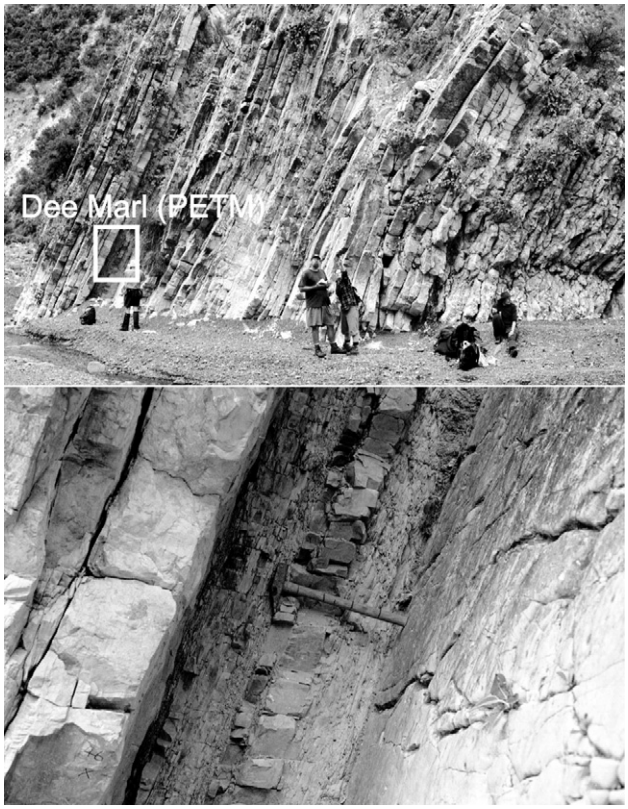

FIGURE 2 | **General (top) and close-up (bottom) photographs of Dee Marl beds at Muzzle Stream.**

Overall compacted sedimentation rates for upper Paleocene and lower Eocene sediments at the three sections (Table 1) can be determined according to several biostratigraphic and carbon isotope datums (Hollis et al., 2005a, b).

Samples were exhumed from rocks at each section using a hammer and chisel. In total, 34, 41 and 19 samples were obtained from Mead Stream, Dee Stream and Muzzle Stream, respectively. Given the PETM intervals examined, mean sampling resolution was approximately 15, 12 and 15 cm at the three locations, which correspond to average time resolutions of between 5 and 11 kyr for Mead Stream, 4 and 12 kyr for Dee Stream, and 15 and 30 kyr for Muzzle Stream.

METHODOLOGY

Magnetic measurements were performed at the Paleomagnetism Laboratory of the Complutense University of Madrid (Spain). Bulk magnetic susceptibility (χ) was measured with a KLY-3 Kappabridge (Agico) susceptibility bridge. Due to the low values, each sample was measured ten times and averaged. Hysteresis and remanence cycles were measured with a Coercivity Spectrometer developed by Kazan University (Burov et al., 1986) and sited at Madrid Paleomagnetism Laboratory. Maximum applied magnetic field and field steps were 0.5 T and 0.5 mT, respectively. Each data-point was measured 9 times and averaged. Hysteresis cycles were linearly corrected for the

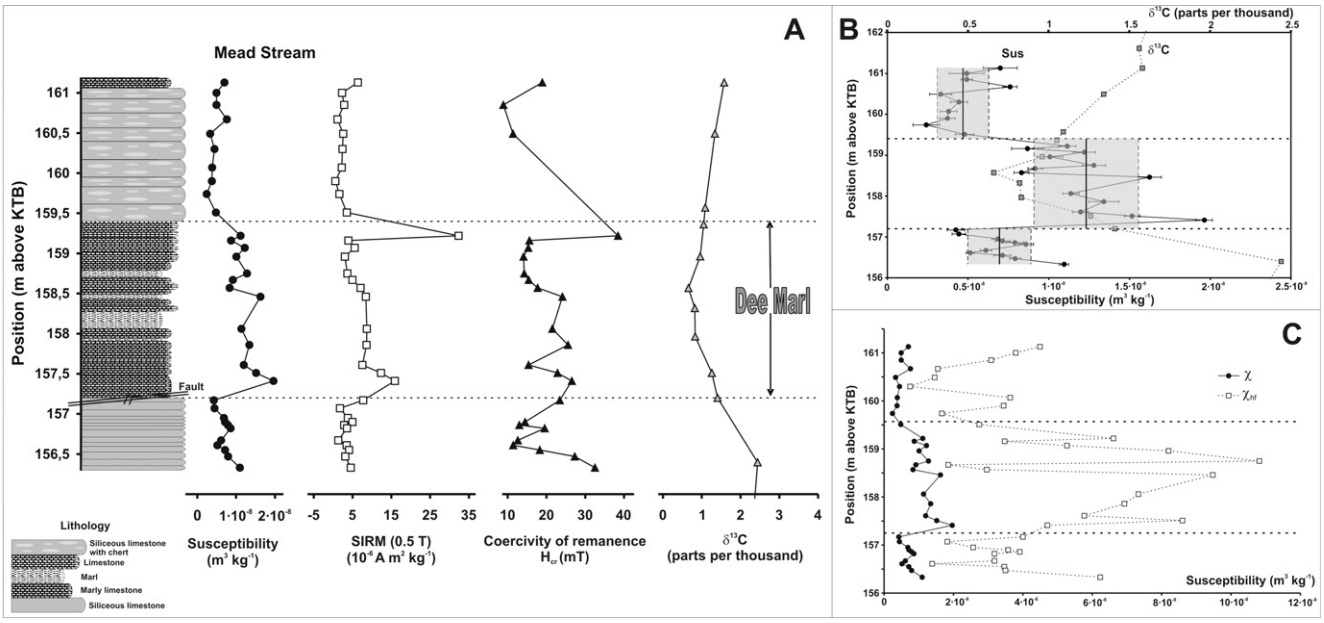

FIGURE 3 | **A) Stratigraphic plot of Mead Stream mass-normalized magnetic susceptibility, SIRM, coercivity of remanence and carbon stable isotope data from Hollis et al. (2005a). B) Magnetic susceptibility and carbon isotopic data plot together for better comparison. Mean susceptibility values (vertical black lines) and standard deviation (grey shades) for samples below, inside and above Dee Marl are also shown. C) Initial low field (χ) and high field (χ_{hf}) magnetic susceptibilities plotted together.**

paramagnetic contribution and high field susceptibility (χ_{hf}), the slope of the linear trend above 0.4 T, was calculated as an estimation of the importance of the paramagnetic fraction. All magnetic measurements were performed at room temperature.

Variations in three main magnetic parameters are summarized in stratigraphic plots, together with previously published stable carbon isotope data (Figs. 3, 4 and 5). These parameters are: bulk magnetic susceptibility; saturation isothermal remanent magnetization, or SIRM (the remanent magnetization acquired by the sample under the maximum applied magnetic field of 0.5 T); and coercivity of remanence, or H_{cr} (the point where the back-demagnetization IRM curve intersects the x-axis, corresponding to the back magnetic field that has to be applied to eliminate the SIRM acquired previously). Susceptibility and SIRM were normalized by sample mass. Due to the very low ferromagnetic concentration in some samples, especially at Mead Stream, it was not possible to determine H_{cr} with any confidence. For those samples, no value is plotted, and this is the reason for the lower resolution in the Mead Stream H_{cr} profile.

RESULTS

Mead Stream

Bulk magnetic susceptibility averages about $7{\cdot}10^{-9}$ m^3kg^{-1} before the PETM, rises to $12{\cdot}10^{-9}$ m^3kg^{-1} across Dee Marl, and drops to $5{\cdot}10^{-9}$ m^3kg^{-1} above (Table 2 and Fig. 3). This record has a clear overall negative correlation with the bulk carbonate $\delta^{13}C$ record (Fig. 3B). We note, however, two seemingly important observations. Sediment within Dee Marl shows significant variations in magnetic susceptibility. Sediment above Dee Marl has lower bulk magnetic susceptibility than below this unit, even though $\delta^{13}C$ values are less.

The increase in magnetic susceptibility across Dee Marl is tracked by an overall increase in SIRM, that averages about $3.8{\cdot}10^{-6}$ Am^2kg^{-1} before the PETM, rises to $9.4{\cdot}10^{-6}$ Am^2kg^{-1} across Dee Marl (or $7.5{\cdot}10^{-6}$ Am^2kg^{-1} if the peak in the upper part of Dee Marl is not included), and drops to $2.6{\cdot}10^{-6}$ Am^2kg^{-1} above (Table 2 and Fig. 3). However, there is an extreme SIRM peak ($32{\cdot}10^{-6}$ Am^2kg^{-1}) near the top of Dee Marl that is not observed in the magnetic susceptibility profile.

Coercivity of remanence data must be considered with caution due to the low ferromagnetic content of the samples. Nonetheless, a general trend is observed (Fig. 3): inside Dee Marl, sediment with higher SIRM has slightly higher H_{cr} (~25 mT), especially the peak in SIRM, which also corresponds to a peak in H_{cr} (~38 mT), than samples with lower SIRM, whose coercivity of remanence is around 15 mT. Above and below Dee Marl H_{cr} values are slightly lower, between 10 and 20 mT, with the exception of the lowermost samples, where values around 30 mT are reached. If mean values below, inside and above Dee

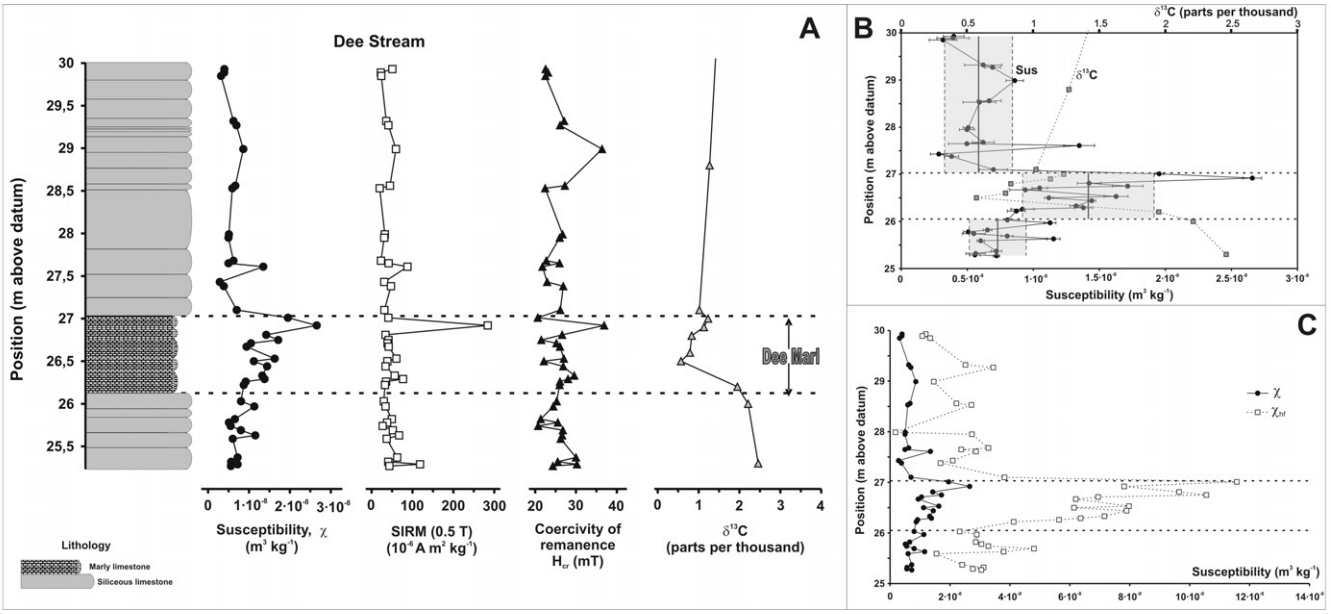

FIGURE 4 | **Stratigraphic plot of Dee Stream mass-normalized magnetic susceptibility, SIRM, coercivity of remanence and carbon stable isotope data from Hancock et al. (2003). B) Magnetic susceptibility and carbon isotopic data plot together for better comparison. Mean susceptibility values (vertical black lines) and standard deviation (grey shades) for samples below, inside and above Dee Marl are also shown. C) Initial low field (χ) and high field (χ_{hf}) magnetic susceptibilities plotted together.**

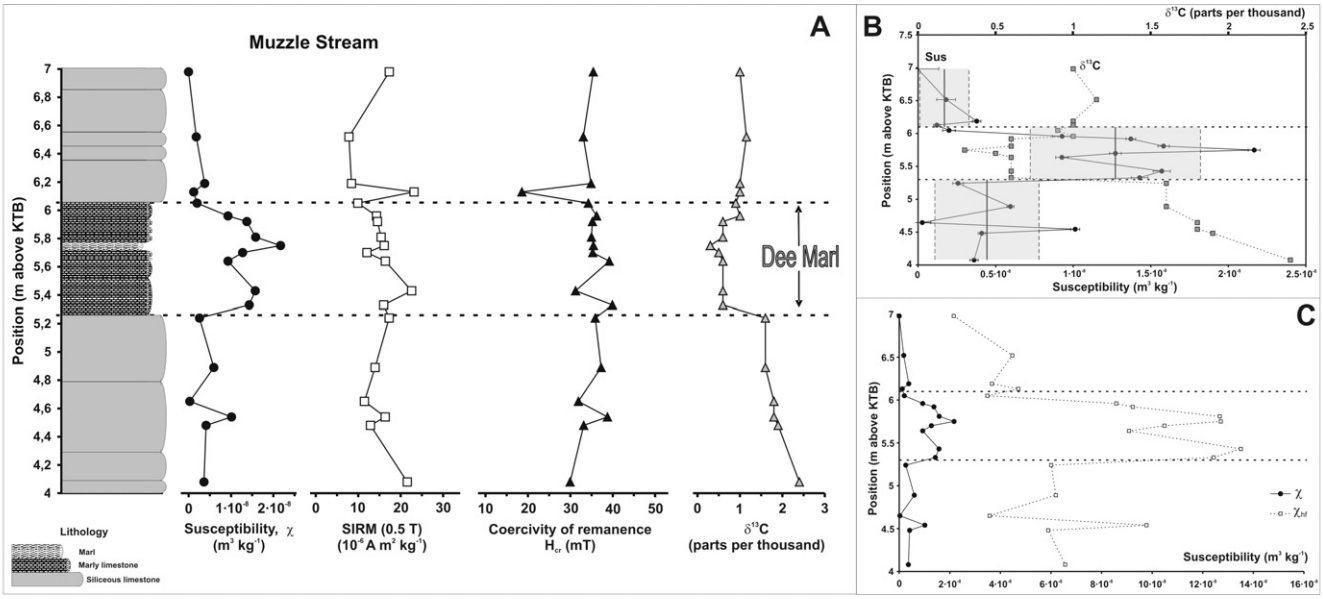

FIGURE 5 | **A) Stratigraphic plot of Muzzle Stream mass-normalized magnetic susceptibility, SIRM, coercivity of remanence and carbon stable isotope data from Hollis et al. (2005b). B) Magnetic susceptibility and carbon isotopic data plot together for better comparison. Mean susceptibility values (vertical black lines) and standard deviation (grey shades) for samples below, inside and above Dee Marl are also shown. C) Initial low field (χ) and high field (χ_{hf}) magnetic susceptibilities plotted together.**

Marl are considered (Table 2), and regarding that there are just 3 samples above Dee Marl where H_{cr} could be calculated with confidence, no significant differences are observed when the high SIRM, high H_{cr} peak of uppermost Dee Marl is removed.

High field susceptibility (χ_{hf}) has been estimated calculating the slope of the linear trend of the hysteresis cycles above 0.4 T. This χ_{hf} is plotted along initial or low field susceptibility (χ) in Fig. 3C, and can be regarded as an estimation of paramagnetic contribution. As can be seen, χ_{hf} is correlated with χ, with a significant increase across Dee Marl.

Dee Stream

The magnetic susceptibility record across the PETM at Dee Stream is generally similar to, although slightly higher, that at Mead Stream. Bulk magnetic susceptibility averages about $7{\cdot}10^{-9}$ m^3kg^{-1} before the PETM, rises to $14{\cdot}10^{-9}$ m^3kg^{-1} across Dee Marl, and drops to $6{\cdot}10^{-9}$ m^3kg^{-1} above (Table 2 and Fig. 4). This record is also negatively correlated with the bulk carbonate $\delta^{13}C$ record (Fig. 4B). Again, as at Mead Stream, sediment within Dee Marl shows significant variations in magnetic susceptibility, and sediment above has slightly lower bulk magnetic susceptibility than below. A noticeable spike in magnetic susceptibility ($27{\cdot}10^{-9}$ m^3kg^{-1}), SIRM ($2.8{\cdot}10^{-4}$ Am^2kg^{-1}) and coercivity of remanence (37 mT) is observed at the 26.92 m mark at Dee Stream (Fig. 4). Similar to the record at Mead Stream, this is near the top of Dee Marl, where $\delta^{13}C$ begins to recover.

Mean SIRM values are $50{\cdot}10^{-6}$ Am^2kg^{-1} before the PETM, $63{\cdot}10^{-6}$ Am^2kg^{-1} across Dee Marl (or $44{\cdot}10^{-6}$ Am^2kg^{-1} if the peak in the upper part of Dee Marl is not included), and $39{\cdot}10^{-6}$ Am^2kg^{-1} above (Table 2, Fig. 4). As can be seen, if the peak in χ, SIRM, and H_{cr} at the upper part of Dee Marl is excluded from the calculations, mean values in SIRM and H_{cr} are approximately the same below, inside and above Dee Marl. These are major differences between Dee Stream and Mead Stream: SIRM is an order of magnitude higher at Dee Stream than at Mead Stream and no significant changes in mean SIRM values are observed across the PETM in Dee Stream.

Concerning coercivity of remanence, higher values of SIRM again generally correspond to values in H_{cr} slightly higher than those of immediately surrounding samples. This is observed in the whole profile, not just inside Dee Marl. To better illustrate the differences in

TABLE 1 | **Mean compacted sedimentation rates in cm/kyr.**

	Upper Paleocene	Dee Marl	Lower Eocene
Mead Stream[a]	2.7	2.4-3	1.4
Dee Stream[b]	2-3	1-1.3	2-3
Muzzle Stream[b]	0.5-0.6	0.8-1	0.5-0.6

a) Hollis et al. (2005a)
b) Hollis et al. (2005b)

TABLE 2 | **Mean values of the magnetic parameters below, inside and above Dee Marl.**

	Mead Stream			Dee Stream			Muzzle Stream		
	χ (m^3kg^{-1})	$SIRM_{0.5\ T}$ (Am^2kg^{-1})	H_{cr} (mT)	χ (m^3kg^{-1})	$SIRM_{0.5\ T}$ (Am^2kg^{-1})	H_{cr} (mT)	χ (m^3kg^{-1})	$SIRM_{0.5\ T}$ (Am^2kg^{-1})	H_{cr} (mT)
Above	$4.7 \cdot 10^{-9}$	$2.56 \cdot 10^{-6}$	13.1	$5.9 \cdot 10^{-9}$	$38.9 \cdot 10^{-6}$	25.4	$1.7 \cdot 10^{-9}$	$14.2 \cdot 10^{-6}$	30.5
Dee marl								**$11.2 \cdot 10^{-6}$**	**34.4**
Inside	$12.3 \cdot 10^{-9}$	$9.39 \cdot 10^{-6}$	20.5	$14.2 \cdot 10^{-9}$	$62.7 \cdot 10^{-6}$	26.4	$12.7 \cdot 10^{-9}$	$15.2 \cdot 10^{-6}$	35.7
Dee marl		**$7.48 \cdot 10^{-6}$**	**19.0**		**$44.3 \cdot 10^{-6}$**	**25.5**			
Below Dee marl	$6.9 \cdot 10^{-9}$	$3.75 \cdot 10^{-6}$	19.2	$7.3 \cdot 10^{-9}$	$49.9 \cdot 10^{-6}$	25.6	$4.4 \cdot 10^{-9}$	$15.6 \cdot 10^{-6}$	34.5

Note: When two values are tabulated, the **bold** one is calculated after rejection of the spike in the upper part of Dee Marl (Mead Stream and Dee Stream) and the spike just overlaying Dee Marl (Muzzle Stream).

H_{cr} at Dee Stream, rescaled and normalized IRM back-demagnetization curves were made for selected lower coercivity and higher coercivity samples (Fig. 6). Despite noise affecting the data, there is a clear and significant difference in the behaviour of these samples. Low-coercivity samples have their coercivity of remanence spectra displaced towards lower magnetic fields. This is observed preferentially in the low-field part of the curves and is expressed as higher curve gradients below 50 mT for low coercivity of remanence samples. This change in shape of the curves between the two types of behaviour is reflected in the coercivity of remanence values. Nevertheless, the differences in H_{cr} are small, with all the values varying between ~20 and 30 mT, with the exception of the peak in the upper part of Dee Marl (37 mT) and another high value at the 29 m mark (36 mT).

As in the case of Mead Stream and despite the higher fraction of ferromagnetic minerals in Dee Stream, deduced from the ten-times higher SIRM values, the hysteresis cycles of Dee Stream samples show also very strong linear trends (see two examples in Fig. 7). Again, χ_{hf} has been estimated calculating the slope of this linear trend above 0.4 T (Fig. 4C). It correlates well with χ and shows a significant increase across Dee Marl.

Muzzle Stream

The magnetic susceptibility profile across the PETM at Muzzle Stream also shows a clear negative correlation to the bulk carbonate $\delta^{13}C$ record. However, the amplitude of the change is greater here than in the other two sections. Bulk magnetic susceptibility averages about $4 \cdot 10^{-9}$ m^3kg^{-1} before the PETM, rises to $13 \cdot 10^{-9}$ m^3kg^{-1} across Dee Marl, and drops to $2 \cdot 10^{-9}$ m^3kg^{-1} above (Table 2 and Fig. 5).

In contrast to Mead Stream, but similarly to Dee Stream, the increase in magnetic susceptibility across Dee Marl is not clearly accompanied by an increase in SIRM. Instead, it is consistently higher than at Mead Stream but lower than at Dee Stream (~$14\text{-}15 \cdot 10^{-6}$ Am^2kg^{-1}).

The H_{cr} profile at Muzzle Stream also differs from that at the other sections (Fig. 5). In almost all Muzzle samples H_{cr} varies between 30 and 40 mT, which contrasts with the 10-30 mT and 20-30 mT measured at

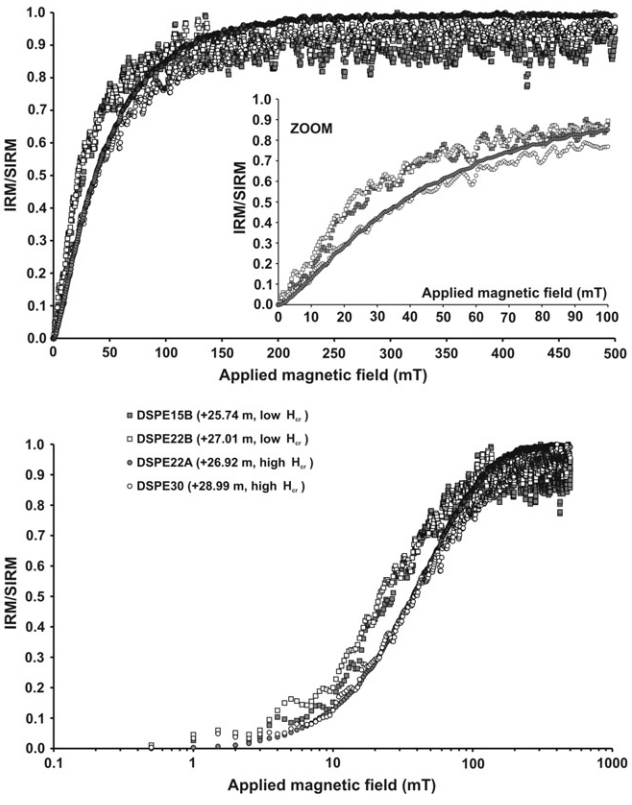

FIGURE 6 | **IRM back-demagnetization curves (rescaled and normalized) for representative Dee Stream samples. Top: linear scales and zoom on the initial part of the curves. Bottom: the same curves plotted with a logarithmic scale in the applied field axis. This scale usually allows a better visualization of the differences in behaviour between samples with high and low coercivity of remanence.**

Mead Stream and Dee Stream, respectively (excepting the "spikes" near the top of Dee Marl). Additionally, the SIRM high value corresponding to the "spike" just overlaying Dee Marl is associated with a low value of H_{cr} (18 mT), whereas the upper-Dee Marl peaks at Mead Stream and Dee Stream show relatively higher H_{cr}.

As in the previous sections, χ_{hf} has been estimated from the hysteresis cycles (Fig. 5C). Again, it correlates well with χ and shows a significant and consistent increase across Dee Marl.

DISCUSSION

Paramagnetic *vs.* ferromagnetic contributions

Several arguments point to a strong control of the susceptibility signal in the studied sections by paramagnetic content. First, the three sections show very similar values of susceptibility, while SIRM vary over one order of magnitude. This indicates that the contribution of the ferromagnetic fraction to the total susceptibility must be small. Second, the clear increase in susceptibility across Dee Marl, observed in all sections and reaching a factor of almost 3, is not correlated with an equally significant increase in SIRM. The only section where both susceptibility and SIRM increase by a factor of ~2 is Mead Stream; in the other two, where average SIRM values are much higher than at Mead Stream, this is not observed. And third, the hysteresis cycles themselves show very strong linear trends, even in Dee Stream samples, which have the highest SIRM values and therefore the highest ferromagnetic contents. The slope of this linear trend, calculated above 0.4 T, allows an estimation of high field susceptibility (controlled by the paramagnetic fraction), showing a strong correlation with initial (low field) susceptibility and similar increases across Dee Marl.

Additional information is obtained from the bilogarithmic plot of susceptibility *versus* SIRM of Fig. 8. The diagonal straight line shown in the figure corresponds to a hypothetical set of samples with increasing quantities of a typical magnetite with SIRM/χ = 10 kA m^{-1}, corresponding to a mean grain size of ~5 microns (Thompson and Oldfield, 1986). Samples above and to the left of this linear trend have very low magnetite and high paramagnetic contributions. The samples of the three studied sections fall in the low-ferrimagnetic, high-paramagnetic content region of the plot, strengthening the conclusion that their susceptibility is strongly controlled by the paramagnetic fraction. The highest values of SIRM are those of Dee Stream samples, which show also a stronger coupling between susceptibility and SIRM, indicating higher ferromagnetic contribution.

Magnetic susceptibility

Magnetic susceptibility is generally very low at all three sections compared to other marine sediments and sedimentary rocks, including other Cretaceous and early Paleogene limestones deposited along continental margins and across epoch boundaries (Fig. 9). Because in the studied sections magnetic susceptibility relates mainly to the abundance of paramagnetic minerals, which typically corresponds to the amount of detrital material in marine sediment, this is consistent with the terrigenous-sediment starved nature of the Marlborough paleo-platform in the Early Paleogene (Crampton et al., 2003).

Across Dee Marl, there is a major increase in bulk magnetic susceptibility at all three sections. When mean values are considered, they rise by a factor of 1.8 at Mead Stream, 2.0 at Dee Stream, and 2.9 at Muzzle Stream. This general increase is consistent with higher amounts of detrital material, as expected from the change in lithology. Importantly, the increase in magnetic susceptibility is greater toward the paleo-coastline. These observations support increased ter-

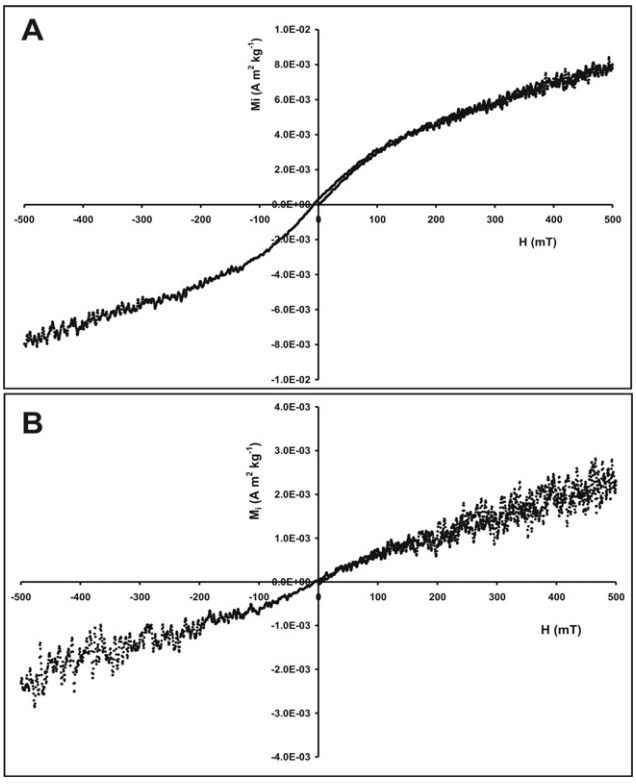

FIGURE 7 | **Hysteresis cycles (induced magnetization versus applied magnetic field) for two Dee Stream samples. A) Sample DSPE22A corresponding to the high SIRM, high Hcr spike at 26.92 m. B) Sample DSPE15B, corresponding to low SIRM, low H_{cr} values at 25.74 m. Note the very important linear trend, and hence paramagnetic contribution, in both samples, but especially in the bottom one. Instrumental high-frequency noise is evident at high magnetic fields due to the relatively low ferromagnetic content of the samples.**

rigenous discharge to this margin during the PETM. This agrees with recent interpretations at these locations (Hancock et al., 2003; Hollis et al., 2005a, b; Nicolo et al., 2007), previous reports from other margins (Schmitz et al., 2001; Crouch et al., 2003; Dickens and Francis, 2004; Giusberti et al., 2007), and generic expectations for high latitude margins during intervals of global warming.

Previous studies on deep-sea cores (Norris and Röhl, 1999; Röhl et al., 2000) have noted 10 or 11 magnetic susceptibility or chemical (e.g., Fe) oscillations across the entire PETM, perhaps related to changes in sediment deposition on the ~21,000 yrs precession cycle. Recently, this also has been observed in bathyal sections along a continental margin now exposed in northern Italy, particularly at Forada (Giusberti et al., 2007). Here, however, only the first 5 or 6 cycles are pronounced. Of the three sections, Mead Stream has the most expanded PETM interval and represents the deepest and most oceanic depositional environment. Consequently, it might be expected to have similar cycles. Although the sampling resolution is poor, we observe variations in magnetic susceptibility across Dee Marl at Mead Stream (Fig. 3) that are consistent with 5-6 cycles.

Studies at other locations, notably Ocean Drilling Program Site 690 and Forada, have also noted a major drop in the abundance of terrigenous material following the initial 80-100 kyrs of the PETM (Kelly et al., 2005; Giusberti et al., 2007). This is consistent with the bulk rock magnetic susceptibility at all three locations in the Clarence Valley, which show a marked drop during the recovery in $\delta^{13}C$ (Figs. 3, 4 and 5). This may represent onset of excess carbonate deposition, as predicted by certain models (e.g., Dickens et al., 1997) and evidenced at ODP Site 690 (Kelly et al., 2005). Likely, it represents both enhanced carbonate accumulation and shutdown of siliciclastic delivery, as inferred at Forada (Giusberti et al., 2007).

Saturation Isothermal Remanent Magnetization

The SIRM directly relates to the ferromagnetic content of the sediment. Background values are very low at Mead Stream ($4 \cdot 10^{-6}$ Am^2kg^{-1}), low at Muzzle Stream ($15 \cdot 10^{-6}$ Am^2kg^{-1}) but relatively higher at Dee Stream ($50 \cdot 10^{-6}$ Am^2kg^{-1}). This directly relates to the ferromagnetic content of sediment at the three sites.

Only at Mead Stream do we observe an average increase in SIRM across Dee Marl very similar in magnitude to the increase in susceptibility. In the other two sections average SIRM remains practically unchanged below and inside Dee Marl, apart from a single peak in the upper part of Dee Marl. In the three sections, average SIRM values above Dee Marl are slightly lower than below Dee Marl. In Dee Stream, although no overall increase in SIRM is observed, the most increases in susceptibility are matched with increases in SIRM and thus in ferromagnetic content. This is also observed, but to a lesser extent, in Mead Stream. In Muzzle Stream the susceptibility variations are not coupled with SIRM variations. In Dee Stream the two parameters are more coupled, as the position of Dee samples in the bilogarithmic plot of Fig. 8 shows. This indicates that: a) the ferromagnetic versus paramagnetic contribution to the magnetic properties is higher in Dee that in Mead or Muzzle; and b) the susceptibility increase within the PETM is mainly controlled by an increase in the paramagnetic fraction, and thus in the terrigenous fraction. This point is in agreement with gamma ray field data from Hollis et al. (2005a).

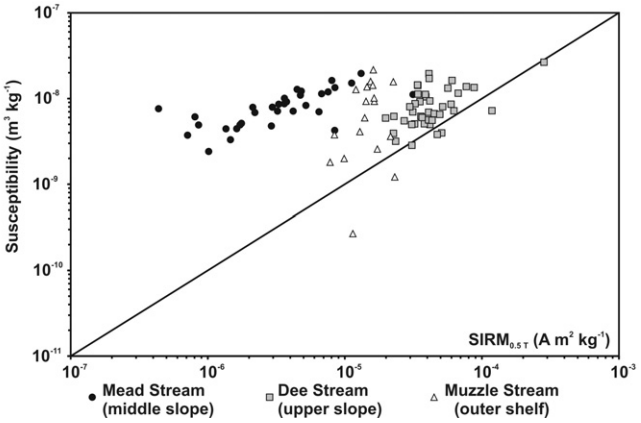

FIGURE 8 | **Bilogarithmic plot of magnetic susceptibility versus SIRM for all the studied samples. The straight line represents the behaviour of a hypothetical set of samples with increasing fractions of a typical magnetite with SIRM/χ = 10 kA m^{-1}, corresponding to a mean grain size of ~5 microns. Samples above and to the left of this trend have very low magnetite and high paramagnetic contributions. Samples below and to the right of the line have increasing contributions from high-coercivity phases.**

Coercivity of remanence

Although caution has to be placed in connection with the coercivity of remanence results due to the low ferromagnetic content and the noisy character of the remanence curves, some remarks can be made. Background H_{cr} varies between 10-30 mT at Mead Stream, 20-30 mT at Dee Stream and 30-40 mT at Muzzle Stream. These values are within those expected for magnetite and similar low-coercivity phases, but the differences are significant and can be explained in terms of varying contributions of high-coercivity phases (e.g., haematite, goethite).

The alternating relative increases in SIRM at Dee Stream and Mead Stream are loosely coupled with

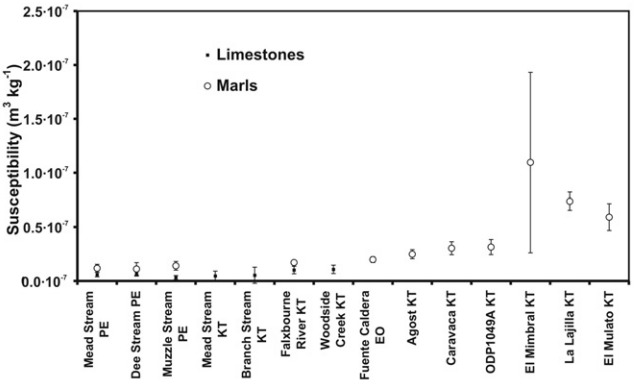

FIGURE 9 | **Mean magnetic susceptibility for limestones and marls from different sections and ages. Standard deviation is also shown as a measure of the internal variation of susceptibility within each group. Sections: Fuente Caldera, Eocene-Oligocene boundary (southern Spain); Agost and Caravaca, K-T boundary (south-eastern Spain); ODP Hole 1049A, K-T boundary (Blake Nose, North Atlantic); El Mimbral, La Lajilla and El Mulato, K-T boundary (north-eastern Mexico); Branch Stream, Flaxbourne River and Woodside Creek are other New Zealand (South Island) K-T boundary sections. Note: when the K-T boundary is concerned, susceptibility data refers to normal end-Cretaceous and lowermost-Paleogene limestones and marls, not to the K-T boundary ejecta layer.**

increases in H_{cr} , reaching values of ~25-30 mT, more similar to the background values in Muzzle. Therefore, these increases are associated in Dee and Mead with relative increases in both the ferromagnetic content and also in the importance of high-coercivity magnetic phases. This tendency is broken at Muzzle, the shallower and most compacted section, where coercivity values remain high and stable, with the exception of the prominent SIRM spike just above Dee Marl. This spike is connected to a significant decrease in H_{cr}.

These observations can be explained also by variable terrigenous input, with sporadic intensification of discharge fluxes, if it is assumed that: a) the terrigenous material weathered from emerged New Zealand sub-continent, mainly composed of paramagnetic minerals (i.e. clays), has some ferromagnetic fraction, presumably a mixture of different minerals, with H_{cr} values displaced towards high coercivity magnetic phases; and b) the ferromagnetic fraction in Dee Stream and Mead Stream sediments was generally more dominated by lower coercivity phases of biogenic and/or diagenetic origin. In Muzzle Stream, located at a shallower, outer shelf setting, the terrigenous contribution, whose ferromagnetic fraction was dominated by higher coercivity phases, was already the controlling factor before, during and after the PETM. With these assumptions, the rock magnetic data are satisfactorily explained, with two exceptions: the high-SIRM, high- H_{cr} spike observed in the upper part of Dee Marl at Dee Stream and Mead Stream; and the high-SIRM, low-H_{cr} spike observed at Muzzle just above Dee Marl.

Although the susceptibility increase across the initial part of the PETM is clearly correlated to increases in terrigenous input, the SIRM and H_{cr} behaviour could be also influenced by changes in diagenetic conditions, possibly connected to the reported drop in redox conditions (Dickens and Francis, 2004). In relation to this, it may be significant to observe that at Mead Stream the upper layers of Dee Marl, roughly between the marks 158.75 m and 159.16 m, showed in the field the presence of some pyrite clusters, possibly indicating the on-set of reducing conditions. Just on top of this pyrite-enriched zone lays the sample at 159.22 m, which shows the prominent peak in SIRM and H_{cr}. In cases where sediments are deposited under anoxic and reducing conditions dissolution, remobilization of elements and alteration of magnetic mineralogy are expected and it is usual to find a top layer with enhanced ferromagnetic content and higher coercivity of remanence, just at the transition from suboxic to oxic conditions (see for example Karlin et al., 1987; Sahota et al., 1995; Tarduno and Wilkinson, 1996; Passier et al., 2001). This could be the case of the magnetic spike in the upper part of Dee Marl at Mead Stream and Dee Stream, and also may explain the lack of a similar spike at Muzzle Stream, which due to its shallow nature may not have been exposed to the same oceanic conditions. Clearly, additional geochemical and high-resolution rock magnetic analyses are necessary to confirm these possibilities.

A cometary impact trigger of the PETM?

As was stated in the introduction, Kent et al. (2003) proposed a cometary impact as a trigger mechanism for the onset of the PETM. This scenario was further ellaborated by Cramer and Kent (2005). In their view, a cometary source of light carbon would account for the first steps of the $\delta^{13}C$ decrease, as well as provoking an initial warming that would subsequently lead to gas hydrate destabilization and release. Their guesses about the impactor size vary between 8 and 11 km, with an average size of 10 km considered reasonable by those authors, very similar to the Cretaceous-Tertiary boundary impactor. This impact hypothesis was based in two points: the reported occurrence of a small Ir anomaly (133 ppt, background values of 38 ppt) coincident with the beginning of the PETM $\delta^{13}C$ excursion at Zumaya section, Spain (Schmitz et al., 1997); and the presence of single domain magnetite grains with M_{rs}/M_s ratios between 0.3 and 0.4, considered anomalously high by the authors and corresponding to a narrow size range between 30 and 100 nm, in a kaolinite enriched layer ~5 to 8 m thick deposited in three sections (Ancora, Bass River and Clayton) of the New Jersey Atlantic continental shelf. Kent et al. (2003) interpreted this kaolinite enriched layer as altered material coming from an eroded and re-deposited impact ejecta layer, and the single domain magnetite as a condensation product of an expanding impact

vapour cloud. To reach the last conclusion, Kent et al. (2003) established an analogy between this single domain magnetite and the iron-nanophase that has been reported from several K-T boundary sections and that was proposed as a direct impact-generated phase or even as the K-T boundary iridium carrier (Wdowiak et al., 2001; Verma et al., 2001; Bhandari et al., 2002).

Later, Lippert et al. (2004, 2007) investigated the rock magnetic properties across the PETM in three additional sections: Wilson Lake, also in the New Jersey continental shelf; ODP Site 1262 in Walvis Ridge, South Atlantic; and Lodo, California continental shelf. In Wilson Lake they found results similar to those of Kent et al. (2003), but in the other two sections the magnetic properties were different, not showing the presence of the high M_{rs}/M_s ratio single domain magnetite. They concluded that this New Jersey continental shelf magnetite should be a regional and purely terrestrial component, pointing to a bacterially-mediated biogenic origin, in agreement with the alternative explanation of Dickens and Francis (2003). A bacterial origin for this single-domain magnetite is also supported by Kopp et al. (2007).

The results presented in this paper about three New Zealand sections show not a single trace of the anomalous single domain magnetite reported by Kent et al. (2003), and therefore they serve to strengthen the conclusion that it constitutes a regional characteristic of the New Jersey Atlantic Coastal Plain. In Fig. 10, M_{rs}/M_s ratios for Dee Stream and Muzzle Stream are shown. One has to keep in mind that the low ferromagnetic content and high relative paramagnetic contribution in our sections seriously affect the goodness and noisy character of the hysteresis cycles, making it difficult to properly correct them for the paramagnetic contribution and to calculate hysteresis parameters like M_s and H_c. This is the reason for not showing values for Mead Stream and for including in the figure error bars, corresponding to the propagation of the errors associated mainly with M_s estimation. As can be seen, M_{rs}/M_s ratio remains unchanged through the entire PETM profiles, varying between 0.025 and 0.15, and even considering the error estimations it does not reach the values reported from the New Jersey continental shelf. Of the three studied sections, Muzzle Stream corresponds to an outer shelf setting and therefore should behave similarly to New Jersey continental shelf sections, but it does not. Additionally, our three sections do show an important increase in terrigenous (clay) content coinciding with the onset and initial recovery of the PETM carbon isotopic excursion, as many other sections around the world, but it is not connected with rock magnetic properties indicative of anomalous, impact-derived material. The best interpretation of the enrichment in clay content is therefore an increase in continental weathering and erosion, connected to an acceleration of the hydrological cycle.

Apart from the absence of evidence for a PETM impact in the studied New Zealand sections, some additional and important considerations can be made. First, it seems unreasonable to expect an impact-derived clay-rich layer, re-deposited or not, several meters thick, as Kent et al. (2003) claim. In the case of the K-T boundary impact, with an impactor size of ~10 km, there is not such a layer. The greatest thicknesses, up to several m, are found close to the impact point and correspond to proximal ejecta and/or to siliciclastic high-energy beds emplaced by impact-triggered tsunamis or by sediment gravity flows (Bohor, 1996; Bralower et al., 1998; Smit, 1999; Claeys et al., 2002), and in those cases a great number of impact markers are also present, which appears to not be the case in the sections studied by Kent et al. (2003). Secondly, there are additional problems with the relationship proposed by Kent et al. (2003) between the single domain magnetite and the K-T boundary iron-nanophase. The goethite/haematite nanoparticles detected by means of Mössbauer spectroscopy by Brooks et al. (1985), Wdowiak et al. (2001), Verma et al. (2001) and Bhandari et al. (2002) are characterized by a superparamagnetic behaviour and reach up to 25 nm in estimated size, significantly less that the 30-100 nm sized particles detailed by Kent et al. (2003). Additionally, the rock magnetic properties

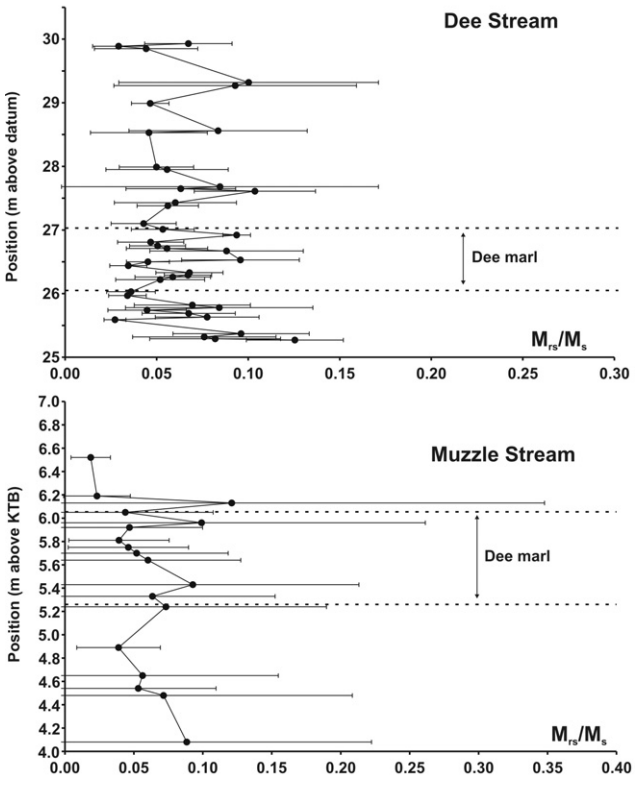

FIGURE 10 **Estimated M_{rs}/M_s ratio across the PETM in Dee Stream and Muzzle Stream.**

exhibited by the layer in which this K-T boundary iron-nanophase is embedded are completely different from those of the New Jersey continental shelf magnetite (Villasante-Marcos et al., 2007). Moreover, the meteoritic nature of this K-T iron-rich nanophase is far from being established, with some authors having interpreted it, at least in some sections, as a diagenetic product (Brooks et al., 1985; Villasante-Marcos et al., 2007).

Many K-T boundary sections do contain an iron phase of Mg, Ni-rich spinels (magnesioferrites) in the fireball layer, whose meteoritic nature has been established on firm grounds. These spinels are thought to have formed as either condensation products in the impact vapour cloud (Bohor et al., 1986; Ebel and Grossman, 2005) or as ablation products from meteoritic fragments (Robin et al., 1992; Gayraud et al., 1996). But their typical size range (up to several microns) and rock magnetic properties (low coercivities and multidomain behaviour) are very different from those of the New Jersey continental shelf single domain magnetite (Worm and Banerjee, 1987; Cisowski, 1988, 1990; Villasante-Marcos et al., 2007). There is no magnetic evidence of the presence of similar Mg, Ni-rich spinels at the three New Zealand PETM sections studied here.

Our results and the above arguments place serious doubt on the PETM comet trigger theory (Kent et al., 2003). To the scope and resolution of this work there is no evidence in the three high-latitude South Pacific margin sections we studied that an impact of significant magnitude occurred at the Paleocene/Eocene boundary. Further, all reported rock magnetic properties are best explained by an endogenous process such as enhanced detrital terrigenous deposition.

CONCLUSIONS

Rock magnetic data across the PETM in the three studied sections from Clarence River valley support the following paleoenvironmental interpretations. During the latest Paleocene, the three locations accumulated sediment across the northern continental margin of New Zealand, a high southern latitude terrigenous-starved sedimentary setting. The shallowest site on the outer shelf (Muzzle Stream) received relatively more weathered and eroded material from land and relatively less biogenic material from the water column compared to the deepest site on the upper slope (Mead Stream). Thus, Muzzle Stream SIRM values were higher than those recorded at Mead Stream, and the ferromagnetic fraction was dominated by detrital minerals with coercivities of remanence >30 mT. At Dee Stream, whose sediments were deposited at an intermediate depth, the terrigenous contribution was minor and the biogenic or diagenetic production was responsible for a lower coercivity (<30 mT) ferromagnetic fraction. A similar interpretation applies to Mead Stream, which recorded even lower terrigenous and biogenic/diagenetic contributions.

Following the onset of the PETM, erosion and likely weathering of the adjacent continent increased, so that more terrigenous material was discharged to the margin. This material was composed mainly of paramagnetic minerals (clays), as indicated by elevated magnetic susceptibility at all sites but most pronounced at Muzzle Stream, the nearest section to the paleo-coastline. Further, these sediments contained an elevated amount of ferromagnetic minerals with relatively high remanence coercivities. However, this overall increase in terrestrial discharge varied, resulting in significant fluctuations in magnetic susceptibility and SIRM.

Above Dee Marl, during the carbon isotopic excursion recovery interval, which initiated ~80-100 kyrs post PETM onset, magnetic susceptibility and SIRM values suddenly decrease and become slightly lower than those of the latest Paleocene. This represents a decrease in the concentration of terrigenous material resulting from either 1) a shutdown of siliciclastic delivery to the New Zealand continental margin, 2) an increase in biogenic carbonate deposition, or 3) some combination of these factors.

ACKNOWLEDGEMENTS

We thank Richard and Sue Murray for permitting us to access these spectacular sections. We are grateful to New Zealand GNS Science Staff and sample curation facilities, especially John Simes. We also thank Percy Strong, James Crampton, John Simes and Lucıa Lozano for their collaboration during fieldwork in the Clarence Valley. We are grateful to Jaume Dinarès-Turrell and an anonymous referee for their useful reviews. This work has been partially funded through a travel grant to V. Villasante-Marcos, from the Universidad Complutense de Madrid (Spain). Participation by G. Dickens and M. Nicolo was funded through an NSF Biocomplexity Grant. C. J. Hollis acknowledges the support of the NZ Foundation for Research, Science and Technology through the GNS Global Change Through Time programme.

REFERENCES

Allen, M.R., Ingram, W.J., 2002. Constraints on future changes in climate and the hydrologic cycle. Nature, 419, 224-232.

Bhandari N., Verma H.C., Upadhyay, C., Tripathi, A., Tripathi, R.P., 2002. Global occurrence of magnetic and superparamagnetic iron phases in Cretaceous-Tertiary boundary clays. In: Koeberl, C., MacLeod, K.G. (eds.). Catastrophic events and mass extinctions: impacts and beyond. Geological Society of America Special Paper, 356, 201-211.

Bice, K.L., Marotzke, J., 2002. Could changing ocean circulation have destabilized methane hydrate at the Paleocene/Eocene boundary? Paleoceanography, 17(2): 10.1029/2001PA000678.

Bohor, B.F., 1996. A sediment gravity flow hypothesis for siliciclastic units at the K/T boundary, northeastern Mexico. In: Ryder, G., Fastovsky, D., Gartner, S. (eds.). The Cretaceous-Tertiary boundary event and other catastrophes in Earth History. Geological Society of America, Special Paper, 307, 183-195.

Bohor, B.F., Foord, E.E., Ganapathy, R., 1986. Magnesioferrite from the Cretaceous-Tertiary boundary, Caravaca, Spain. Earth and Planetary Science Letters, 81, 57-66.

Bowen, G.J., Bralower, T.J., Delaney, M.L., Dickens, G.R., Kelly, D.C., Koch, P.L., Kump, L.R., Meng, J., Sloan, L.C., Thomas, E., Wing, S.L., Zachos, J.C., 2006. Eocene hyperthermal event offers insight into greenhouse warming. Eos, Transactions, American Geophysical Union, 87(17), 165-169.

Bralower, T.J., Paull, C.K., Leckie, R.M., 1998. The Cretaceous-Tertiary boundary cocktail: Chicxulub impact triggers margin collapse and extensive sediment gravity flows. Geology, 26, 331-334.

Brooks, R.R., Hoek, P.L., Reeves, R.D., Wallace, R.C., Johnston, J.H., Ryan, D.E., Holzbecher, J., Collen, J.D., 1985. Weathered spheroids in a Cretaceous/Tertiary boundary shale at Woodside Creek, New Zealand. Geology, 13, 738-740.

Burov, B., Nurgaliev, D.K., Jasonov, P.G., 1986. Paleomagnetic Analysis. Kazan University Press (in Russian), 176 pp.

Cisowski, S.M., 1988. Magnetic properties of K/T and E/O microspherules: origin by combustion? Earth and Planetary Science Letters, 88, 193-208.

Cisowski, S.M., 1990. The significance of magnetic spheroids and magnesioferrite occurring in K/T boundary sediments. In: Sharpton, V.L., Ward, P.D. (eds.). Global catastrophes in Earth history: An interdisciplinary conference on impacts, volcanism and mass mortality. Geological Society of America, Special Paper, 247, 359-365.

Claeys, P., Kiessling, W., Alvarez, W., 2002. Distribution of Chicxulub ejecta at the Cretaceous-Tertiary boundary. In: Koeberl, C., MacLeod, K.G. (eds.). Catastrophic events and mass extinctions: impacts and beyond. Geological Society of America, Special Paper, 356, 55-68.

Cramer, B.S., Kent, D.V., 2005. Bolide summer: The Paleocene/Eocene thermal maximum as a response to an extraterrestrial trigger. Palaeogeography, Palaeoclimatology, Palaeoecology, 224, 144-166.

Crampton, J., Laird, M., Nicol, A., Townsend, D., Van Dissen, R., 2003. Palinspastic reconstructions of southeastern Marlborough, New Zealand, for mid-Cretaceous-Eocene times. New Zealand Journal of Geology and Geophysics, 46, 153-175.

Crouch, E.M., Dickens, G.R., Brinkhuis, H.E.G., Aubry, M.P., Hollis, C.J., Rogers, K.M., Visscher, H., 2003. The *Apectodinium* acme and terrestrial discharge during the Paleocene-Eocene thermal maximum: new palynological, geochemical and calcareous nannoplankton observations at Tawanui, New Zealand. Palaeogeography, Palaeoclimatology, Palaeoecology, 194, 387-403.

Dickens, G.R., 1999. The blast in the past. Nature, 401, 752-755.

Dickens, G.R., Francis, J.M., 2004. A case for a comet impact trigger for the Paleocene/Eocene thermal maximum and carbon isotope excursion; discussion [modified]. Earth and Planetary Science Letters, 217, 197-200.

Dickens, G.R., Castillo, M.M., Walker, J.C.G., 1997. A blast of gas in the latest Paleocene: Simulating first order effect of massive dissociation of ocean methane hydrate. Geology, 25, 259-262.

Ebel, D.S., Grossman, L., 2005. Spinel-bearing spherules condensed from the Chicxulub impact-vapor plume. Geology, 33, 293-296.

Evans, M.E., Heller, F., 2003. Environmental magnetism. Principles and applications of enviromagnetics. Academic Press, 299 pp.

Gayraud, J., Robin, E., Rocchia, R., Froget, L., 1996. Formation conditions of oxidized Ni-rich spinel and their relevance to the K/T boundary event. In: Ryder, G., Fastovsky, D., Gartner, S. (eds.). The Cretaceous-Tertiary boundary event and other catastrophes in Earth History. Geological Society of America, Special Paper, 307, 425-443.

Giusberti, L., Rio, D., Agnini, C., Backman, J., Fornaciari, E., Tateo, F., Oddone, M., 2007. Mode and Tempo of the Paleocene-Eocene Thermal Maximum in an expanded section from the Venetian Pre-Alps. Geological Society of America Bulletin, 119, 391-412.

Hancock, H.J.L., Dickens, G.R., Strong, C.P., Hollis, C.J., Field, B.D., 2003. Foraminiferal and carbon isotope stratigraphy through the Paleocene-Eocene transition at Dee Stream, Marlborough, New Zealand. New Zealand Journal of Geology and Geophysics, 46, 1-19.

Hollis, C.J., Dickens, G.R., Field, B.D., Jones, C.M., Strong, C.P., 2005a. The Paleocene-Eocene transition at Mead Stream, New Zealand: a southern Pacific record of early Cenozoic global change. Palaeogeography, Palaeoclimatology, Palaeoecology, 215, 313-343.

Hollis, C.J., Field, B.D., Jones, C.M., Strong, C.P., Wilson, G.J., Dickens, G.R., 2005b. Biostratigraphy and carbon isotope stratigraphy of uppermost Cretaceous-lower Cenozoic Muzzle Group in middle Clarence valley, New Zealand. Journal of the Royal Society of New Zealand, 35, 345-383.

Karlin, R., Lyle, M., Heath, G.R., 1987. Authigenic magnetite formation in suboxic marine sediments. Nature, 326, 490-493.

Kelly, D.C., Zachos, J.C., Bralower, T.J., Schellenberg, S.A., 2005. Enhanced terrestrial weathering/runoff and surface ocean carbonate production during the recovery stages of the Paleocene-Eocene thermal maxium. Paleoceanography, 20, PA4023, doi:10.1029/2005PA00113.

Kent, D.V., Cramer, B.S., Lanci, L., Wang, D., Wright, J.D., Van der Voo, R., 2003. A case for a comet impact trigger for the Paleocene/Eocene thermal maximum and carbon isotope excursion. Earth and Planetary Science Letters, 211, 13-26.

Kopp, R.E., Raub, T.D., Schumann, D., Hojatollah, V., Smirnov, A.V., Kirschvink, J.L., 2007. Magnetofossil spike during the

Paleocene-Eocene Thermal Maximum: Ferromagnetic resonance, rock magnetic and electron microscopy evidence from Ancora, New Jersey, USA. Paleoceanography, 22 PA4103.

Lippert, P.C., Zachos, J., Bohaty, S., Quattlebaum, T., 2004. Rock magnetic properties across Paleocene-Eocene boundary sediments from the North Atlantic, South Atlantic and eastern Pacific. Eos Trans AGU, 85(47), Fall Meet. Suppl. Abstract GP31B-0840.

Lippert, P.C., Zachos, J.C., 2007. A biogenic origin for anomalous fine-grained magnetic material at the Paleocene-Eocene boundary at Wilson Lake, New Jersey. Paleoceanography, 22, PA4104.

Maher, B.A., Thompson, R. (eds.), 1999. Quaternary climates, environments and magnetism. Cambridge, Cambridge University Press, 390 pp.

Nicolo, M.J., Dickens, G.R., Hollis, C.J., Zachos, J.C., 2007. Multiple early Eocene hyperthermals: Their sedimentary expression on the New Zealand continental margin and in the deep-sea. Geology.

Norris, R.D., Röhl, U., 1999. Carbon cycling and chronology of climate warming during the Paleocene/Eocene transition. Nature, 401, 775-778.

Pagani, M., Pedentchouk, N., Huber, M., Sluijs, A., Schouten, S., Brinkhuis, H., Sinninghe Damste, J.S., Dickens, G.R., and the IODP Expedition 302 Expedition Scientists, 2006. Arctic hydrology during global warming at the Palaeocene-Eocene thermal maximum. Nature, 442, 671-675.

Passier, H.F., de Lange, G.J., Dekkers, M.J, 2001. Magnetic properties and geochemistry of the active oxidation front and the youngest sapropel in the eastern Mediterranean Sea. Geophysical Journal International, 145, 604-614.

Ravizza, G., Norris, R.N., Blusztajn, J., Aubry, M.P., 2001. An osmium isotope excursion associated with the late Paleocene thermal maximum; evidence of intensified chemical weathering. Paleoceanography, 16, 155-163.

Reay, M.B., 1993. Geology of the middle part of the Clarence Valley. Institute of Geological and Nuclear Sciences Geological Map 10, 1-144.

Robert, C., Kennett, J.P., 1992. Paleocene and Eocene kaolinite distribution in the South Atlantic and Southern Ocean; Antarctic climatic and paleoceanographic implications. Marine Geology, 103, 99-110.

Robert, C., Kennett, J.P., 1994. Antarctic subtropical humid episode at the Paleocene-Eocene boundary: clay-mineral evidence. Geology, 22, 211-214.

Robin, E., Bonte, P., Froget, L., Jehanno, C., Rocchia, R., 1992. Formation of spinels in cosmic objects during atmospheric entry: a clue to the Cretaceous-Tertiary boundary event. Earth and Planetary Science Letters, 108, 181-190.

Röhl, U., Bralower, T.J., Norris, R.D., Wefer, G., 2000. New chronology for the late Paleocene thermal maximum and its environmental implications. Geology, 28, 927-930.

Sahota, J.T.S., Robinson, S.G., Oldfield, F., 1995. Magnetic measurements used to identify paleoxidation fronts in deep-sea sediments from the Madeira Abyssal Plain. Geophysical Research Letters, 22, 1961-1964.

Schmitz, B., Pujalte, V., Nunez-Betelu, K., 2001. Climate and sea-level perturbations during the Initial Eocene Thermal Maximum; evidence from siliciclastic units in the Basque Basin (Ermua, Zumaia and Trabakua Pass), northern Spain. Palaeogeography, Palaeoclimatology, Palaeoecology, 165, 299-320.

Smit, J., 1999. The global stratigraphy of the Cretaceous-Tertiary boundary impact ejecta. Annual Review of Earth and Planetary Science, 27, 75-113.

Strong, C.P., Hollis, C.J., Wilson, G.J., 1995. Foraminiferal, radiolarian, and dinoflagellate biostratigraphy of Late Cretaceous to middle Eocene pelagic sediments (Muzzle Group), Mead Stream, Marlborough, New Zealand. New Zealand Journal of Geology and Geophysics, 38, 171-209.

Svensen, H., Planke, S., Malthe-Sorenssen, A., Jamtveit, B., Myklebust, R., Eidem, T.R., Rey, S.S., 2004. Release of methane from a volcanic basin as a mechanism for initial Eocene global warming. Nature, 429, 542-545.

Tarduno, J.A., Wilkinson, S.L., 1996. Non-steady state magnetic mineral reduction, chemical lock-in and delayed remanence acquisition in pelagic sediments. Earth and Planetary Science Letters, 144, 315-326.

Thompson, R., Oldfield, F., 1986. Environmental magnetism. London, Allen & Unwin, 227 pp.

Verma, H.C., Upadhyay, Y.C., Tripathi, R.P., Tripathi, A., Shukla, A.D., Bhandari, N., 2001. Nano-sized iron phases at the K/T and P/T boundaries revealed by Mössbauer spectroscopy. Lunar and Planetary Science Conference XXXII, LPI contribution #1270.

Verosub, K.L, Roberts, A.P., 1995. Environmental magnetism: Past, present and future. Journal of Geophysical Research, 100(B2), 2175-2192.

Villasante-Marcos, V., Martınez-Ruiz, F., Osete, M.L., Urrutia-Fucugauchi, J., 2007. Magnetic characterization of Cretaceous-Tertiary boundary sediments. Meteoritics and Planetary Science, 42, 1505-1528.

Walden, J., Oldfield, F., Smith, J. (eds.), 1999. Environmental magnetism. A practical guide. Technical Guides no. 6, London, Quaternary Research Association, 243 pp.

Wdowiak. T.J., Armendarez. L.P., Agresti. D.G., Wad, E.M.L., Wdowiak, S.Y., Claeys, P., Izett, G., 2001. Presence of an iron-rich nanophase material in the upper layer of the Cretaceous-Tertiary boundary clay. Meteoritics and Planetary Science, 36, 123-133.

Worm, H.U., Banerjee, S.K., 1987. Rock magnetic signature of the Cretaceous-Tertiary boundary. Geophysical Research Letters, 14, 1083-1086.

Manuscript received July 2007;
revision accepted December 2007;
published Online October 2008.